*American Mineralogist, Volume 67, pages 826–832, 1982*

# The cation distribution in synthetic $(Fe,Mn)_3(PO_4)_2$ graftonite-type solid solutions

ANDERS G. NORD

*Section of Mineralogy, Swedish Museum of Natural History*
*P.O. Box 50007, S-104 05 Stockholm 50, Sweden*

AND TORE ERICSSON

*Department of Mineralogy and Petrology*
*Institute of Geology, University of Uppsala*
*P.O. Box 555, S-751 22 Uppsala, Sweden*

**Abstract**

Nine $(Fe_{1-x}Mn_x)_3(PO_4)_2$ solid solutions ($0.1 \leq x \leq 0.9$) with the graftonite-type structure have been prepared and equilibrated at 1070 K. The structure contains three distinct cation coordination polyhedra, all distorted: one octahedron, and two five-coordinated polyhedra. Accurate unit cell dimensions ($P2_1/c$) have been obtained from Guinier–Hägg photographic data for these phases. Mössbauer spectra in combination with a neutron diffraction study of $(Fe_{0.50}Mn_{0.50})_3(PO_4)_2$ have been used to determine the cation distribution for the various compositions. $Mn^{2+}$ preferentially enters the distorted octahedra and $Fe^{2+}$ the five-coordinated sites. The site populations obtained are in agreement with general cation preference trends.

## Introduction

Many studies have been performed with the aim of determining how approximately equidimensional cations distribute themselves among distinct crystallographic sites in minerals and inorganic structures. Such studies are principally concerned with important oxysalt structures of natural and synthetic minerals containing ubiquitous elements such as calcium, iron, manganese *etc*. However, only 4-, 6-, and 8-coordinated environments have been investigated in detail so far. Therefore we have started investigations involving five-coordinated sites based on the farringtonite structure type (*e.g.* DuFresne and Roy, 1961; Calvo, 1963; Nord and Kierkegaard, 1968). Some results have already been published (*e.g.* Nord, 1977; Nord and Stefanidis, 1980; Annersten *et al.*, 1980). We now extend our studies to graftonite solid solutions of $Mn_3(PO_4)_2$ in $Fe_3(PO_4)_2$. There are three distinct cation sites in $Fe_3(PO_4)_2$: M(1), M(2), and M(3). M(1) has a distorted octahedral environment, while the two other cations have five-coordinated polyhedra that are distorted and geometrically are somewhere between a trigonal bipyramid and a tetragonal pyramid (Kostiner and Rea 1974). According to the criteria of Stephenson and Moore (1968), $M(3)O_5$ is somewhat closer to a trigonal bipyramid, while the converse is true for $M(2)O_5$. The same situation was found in the isomorphous mineral graftonite with the composition $(Fe_{0.60}Mn_{0.27}Ca_{0.13})_3(PO_4)_2$ (Calvo, 1968). The graftonite structure, though, is unusually flexible so that chemical and structural changes may take place although the basic framework is preserved. For instance, Calvo (1968) found the M(1) cations in his graftonite to be 7-coordinated. We now report on the cation distribution in nine synthetic $(Fe_{1-x}Mn_x)_3(PO_4)_2$ solid solutions, isostructural with $Fe_3(PO_4)_2$. The investigations are based on Mössbauer spectroscopic measurements in combination with X-ray and neutron diffraction data.

## Experimental

$Fe_3(PO_4)_2$ and $Mn_3(PO_4)_2$ were prepared as earlier described (Nord and Kierkegaard, 1980). These batch samples were used for all other preparations. The nine $(Fe_{1-x}Mn_x)_3(PO_4)_2$ solid solutions were made by heating stoichiometric amounts of the two pure orthophosphates in evacuated and sealed silica tubes at 1070 K (800±10°C) for one month and afterwards quenching them in water. X-ray powder diffraction data for each sample were obtained at

0003–004X/82/0708–0826$02.00

room temperature (~ 295 K) using a Guinier-Hägg type focusing camera (monochromatized Cr$K\alpha_1$ radiation, KCl internal standard).

Mössbauer spectra ($^{57}$Fe) were recorded in transmission geometry using a conventional set-up working in constant acceleration mode. The material studied (~ 5 mg Fe per cm$^2$) was thoroughly mixed with lucite powder, heated to 380 K where lucite is melted, and cooled. Mössbauer spectroscopic data were then obtained and analyzed as described by Annersten *et al.* (1980).

Neutron powder diffraction data were collected at room temperature at the STUDSVIK *R*2 reactor (Studsvik, Nyköping, Sweden) from 3 cm$^3$ (~ 10 g) of powdered $(Fe_{0.50}Mn_{0.50})_3(PO_4)_2$ kept in a vanadium cup. A double copper-crystal monochromator in parallel setting was used. The average flux was $10^{10}$ neutrons · m$^{-2}$ · s$^{-1}$ for $\lambda \approx 1.56$Å. Data were collected for $2 \leq \theta \leq 40°$ ($\Delta\theta = 0.04°$) with a total scan time of 12 days.

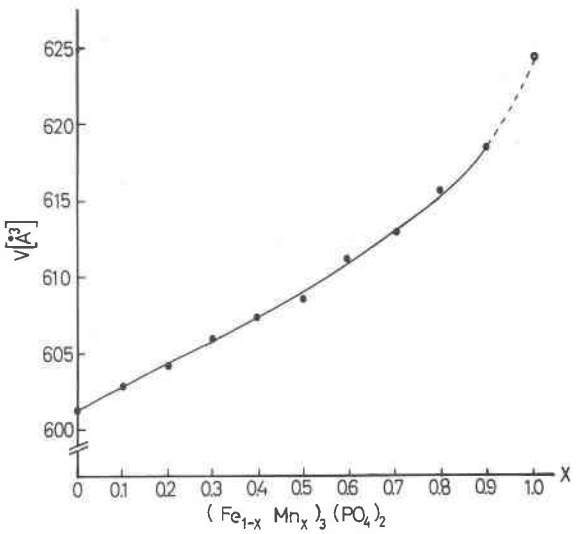


Fig. 1. Unit cell volume $V$ ($Z = 4$) *versus* composition $x$ for $(Fe_{1-x}Mn_x)_3(PO_4)_2$ ($0 \leq x \leq 1$). The value for pure Mn-graftonite (o) is after Stephens (1967).

## X-ray diffraction data

Graftonite and all solid solutions studied herein crystallize in the monoclinic space group $P2_1/c$ (No. 14). Accurate unit cell dimensions were obtained by conventional procedures (programs LAZY and CELREF by A. G. Nord). The cell parameters are listed in Table 1. For clarity, the unit cell volumes *versus* compositions are plotted in Figure 1. The curve $V = f(x)$ for $(Fe_{1-x}Mn_x)_3(PO_4)_2$ obeys Vegard's law up to $x \approx 0.6$, at which point the cell volume increases in a non-linear fashion. This may indicate a change in substitution mechanism as well as presaging the final break-down of the graftonite structure for pure manganese orthophosphate: when quenched from 1070 K, $Mn_3(PO_4)_2$ did not form a graftonite-type structure, but another structure, denoted $\beta'$–$Mn_3(PO_4)_2$ by Stephens and Calvo (1969), occurred.

Table 1. Unit cell dimensions ($P2_1/c$) for $(Fe_{1-x}Mn_x)_3(PO_4)_2$ graftonite-type solid solutions ($0 \leq x \leq 1$) at 295 K

| $x$ | $a$(Å) | $b$(Å) | $c$(Å) | $\beta$(°) | $V$(Å$^3$) |
|---|---|---|---|---|---|
| 0 | 8.882(3) | 11.171(4) | 6.143(2) | 99.31(4) | 601.5(5) |
| 0.10 | 8.863(3) | 11.229(5) | 6.139(3) | 99.25(3) | 603.0(8) |
| 0.20 | 8.842(4) | 11.280(6) | 6.137(2) | 99.15(4) | 604.3(9) |
| 0.30 | 8.829(1) | 11.320(2) | 6.142(1) | 99.15(1) | 606.1(3) |
| 0.40 | 8.819(2) | 11.352(3) | 6.147(1) | 99.14(2) | 607.6(4) |
| 0.50 | 8.810(4) | 11.370(8) | 6.155(3) | 99.07(5) | 608.8(9) |
| 0.60 | 8.806(5) | 11.386(8) | 6.174(3) | 99.00(2) | 611.3(9) |
| 0.70 | 8.803(2) | 11.406(3) | 6.181(1) | 99.00(2) | 613.0(4) |
| 0.80 | 8.804(4) | 11.423(6) | 6.201(2) | 99.00(4) | 615.9(7) |
| 0.90 | 8.803(4) | 11.429(5) | 6.226(2) | 98.97(4) | 618.8(7) |
| 1 *) | 8.81 | 11.45 | 6.27 | 99.0 | 624.7 |

*Figures within parentheses are the standard deviations according to the least-squares procedure*

**) data taken from Stephens (1967)*

## Mössbauer data and analysis

The Mössbauer data are summarized in Table 2 and Figures 2 and 3. The peak positions at room temperature do not change much with the composition $x$ in $(Fe_{1-x}Mn_x)_3(PO_4)_2$. In agreement with the crystal structure, the Mössbauer spectrum is composed of three doublets, giving six partly overlapping lines numbered from 1 to 6 after increasing velocity. The lines 1, 2, and 3 overlap considerably building up the absorption profile on the left in Figure 2. The lines 5 and 6 also overlap each other. It is obvious from Figure 2 that the lines 3 and 4 form one doublet. Furthermore, the computer fits favor a 1-6, 2-5, 3-4 model in agreement with an earlier study of $Fe_3(PO_4)_2$ by Mattievich and Danon (1977).

The resolution of the different $Fe_3(PO_4)_2$ peaks is decreased both at low and at high temperatures as seen in Figure 3. Therefore the Mössbauer analyses of $(Fe_{1-x}Mn_x)_3(PO_4)_2$ were principally performed utilizing the data obtained at room temperature. The model used gives somewhat different intensities for the three doublets in $Fe_3(PO_4)_2$ (*cf.* Table 2), although the three distinct cation sites are occupied by one $Fe^{2+}$ ion; *i.e.*, all iron occupancy factors are equal to unity. This deviation from equal intensities is only partly caused by different Debye temperatures in iron at the three different positions as there

Table 2. Mössbauer parameters for $(Fe_{1-x}Mn_x)_3(PO_4)_2$ ($o \leq x \leq 0.9$)

| $x$ | T(K) | CS (mm/s) | | | $\Delta E_Q$ (mm/s) | | | Intensities | | | $X_{Fe}$ | | | W (mm/s) |
|---|---|---|---|---|---|---|---|---|---|---|---|---|---|---|
| | | M(1) | M(2) | M(3) | M(1) | M(2) | M(3) | M(1) | M(2) | M(3) | M(1) | M(2) | M(3) | |
| 0 | 40 | 1.33 | 1.28 | 1.31 | 2.15 | 1.74 | 2.52 | 0.32 | 0.28 | 0.40 | | | | 0.27 |
| | 78 | 1.31 | 1.25 | 1.29 | 2.19 | 1.72 | 2.54 | 0.34 | 0.28 | 0.39 | | | | 0.29 |
| | 295 | 1.19 | 1.11 | 1.16 | 2.10 | 1.59 | 2.37 | 0.34 | 0.26 | 0.40 | 1*) | 1*) | 1*) | 0.24 |
| | 715 | 0.90 | 0.86 | 0.87 | 1.41 | 1.14 | 1.72 | 0.31 | 0.26 | 0.43 | | | | 0.25 |
| 0.1 | 295 | 1.20 | 1.10 | 1.16 | 2.06 | 1.56 | 2.36 | 0.30 | 0.28 | 0.42 | 0.79 | 0.97 | 0.94 | 0.25 |
| 0.2 | 295 | 1.21 | 1.10 | 1.16 | 2.06 | 1.56 | 2.35 | 0.24 | 0.32 | 0.44 | 0.56 | 0.97 | 0.87 | 0.25 |
| 0.3 | 295 | 1.21 | 1.10 | 1.16 | 2.03 | 1.56 | 2.36 | 0.21 | 0.34 | 0.45 | 0.43 | 0.90 | 0.77 | 0.25 |
| 0.4 | 295 | 1.21 | 1.10 | 1.16 | 2.04 | 1.55 | 2.38 | 0.19 | 0.38 | 0.43 | 0.32 | 0.85 | 0.63 | 0.25 |
| 0.5 | 295 | 1.20 | 1.10 | 1.16 | 2.05 | 1.57 | 2.38 | 0.13 | 0.43 | 0.44 | 0.18 | 0.79 | 0.53 | 0.24 |
| 0.6 | 295 | 1.22 | 1.10 | 1.16 | 2.09 | 1.58 | 2.37 | 0.10 | 0.47 | 0.43 | 0.11 | 0.68 | 0.41 | 0.26 |
| 0.7 | 295 | 1.19 | 1.11 | 1.16 | 2.06 | 1.59 | 2.38 | 0.07 | 0.53 | 0.39 | 0.06 | 0.57 | 0.27 | 0.25 |
| 0.8 | 295 | 1.17 | 1.11 | 1.17 | 1.98 | 1.60 | 2.37 | 0.04 | 0.57 | 0.39 | 0.02 | 0.40 | 0.18 | 0.26 |
| 0.9 | 295 | 1.13 | 1.12 | 1.17 | 1.93 | 1.61 | 2.37 | 0.04 | 0.60 | 0.36 | 0.01 | 0.21 | 0.08 | 0.25 |

*T = absorber temperature in degrees Kelvin. CS = centroid shift measured relative an iron foil at room temperature. $\Delta E_Q$ = quadrupole splitting, i.e., the peak separation in a doublet. $X_{Fe}$ = site occupancies for iron. W = full width at half maximum of the Lorentzian lines, all assumed to be equal in a fit.*

**) All $X_{Fe}$ values have been normalized to equal intensities for $Fe_3(PO_4)_2$ at 295 K.*

*The accuracy of the fitting program is ±0.01 in CS, $\Delta E_Q$, W and intensities.*

is no pronounced temperature dependence in the intensities (Table 2). A combined effect of different Debye temperatures and small amounts (<1 %) of $Fe^{3+}$ and $Fe_2P_2O_7$ impurities may have caused this deviation as will be discussed in a forthcoming paper (Nord and Ericsson, manuscript). Fortunately these effects do not affect the final cation distribution results since the same iron(II) orthophosphate sample was used for all preparations. Moreover, some additional preparations of $Fe_3(PO_4)_2$ were also analyzed, and they gave Mössbauer spectra identical to those shown in Figure 3.

There is a general trend that the centroid shift, CS, increases with coordination number (Clark *et al.*, 1967) as well as with bonding distances (Tang Kai *et al.*, 1980). According to Kostiner and Rea (1974) (all distances mentioned here for $Fe_3(PO_4)_2$ have been taken from that reference) the six-coordinated M(1) site in $Fe_3(PO_4)_2$ has an average Fe–O distance of 2.140Å for the five nearest oxygen atoms and 2.231Å for the six nearest oxygens. The two five-coordinated sites have mean Fe–O distances of 2.134Å [M(2)] and 2.101Å [M(3)]. Consequently it is reasonable to attribute the doublet with the highest CS value (1.19 mm/s at room temperature for $Fe_3(PO_4)_2$) to M(1). For comparison, the "$\gamma$-$Zn_3(PO_4)_2$" structure contains one five- and one six-coordinated cation site with average metal-oxygen distances of 2.05 and 2.15Å, respectively (Calvo, 1963, and personal communication, 1973). The CS values at room temperature for the iron-containing solid solution $\gamma$-$(Zn_{0.90}Fe_{0.10})_3(PO_4)_2$ are 1.11 mm/s for the five- and 1.26 mm/s for the six-coordinated cation site (Annersten *et al.*, 1980).

The two nearest oxygen atoms are much closer for M(2) (1.938 and 1.942Å) than for M(3) (1.996 and 2.042Å). Furthermore, the spread in Fe–O distances for the five oxygen neighbors is much larger for M(2) (0.482Å) than for M(3) (0.234Å). According to Ingalls (1964) the quadrupole splitting, $\Delta E_Q$, for ferrous iron tends to decrease when the distortion, exceeding a threshold value, increases. Thus it seems reasonable to attribute the smallest CS value as well as the smallest $\Delta E_Q$ value to M(2). Accordingly, we attribute CS/$\Delta E_Q$ = 1.11/1.59 (in mm/s units) for $Fe_3(PO_4)_2$ at room temperature to M(2), and 1.16/2.37 to M(3) (*cf.* Table 2). This assignment may seem to be in contradiction to Bancroft's (1973) empirical relationship that the quadrupole splitting increases with the coordination number ($\Delta E_Q$ for M(1) is 2.10 mm/s). However, Bancroft's hypothesis was principally based on 4-, 6-, and 8-coordinated iron sites. Furthermore, the distortion seems to be more pronounced for M(1) with a spread in Fe–O distances of 0.699Å than for M(3), where the spread is only 0.234Å. Mössbauer studies of some $\gamma$-$(Zn_{1-x}Fe_x)_3(PO_4)_2$ solid solutions have also shown that $\Delta E_Q$ for the five-coordinated $Fe^{2+}$ was larger than for the six-coordinated $Fe^{2+}$ (Annersten *et al.*, 1980).

The Mössbauer data for the $(Fe,Mn)_3(PO_4)_2$ solid solutions in combination with the assignment made above indicate that manganese concentrates at the six-coordinated M(1) sites (*cf.* Table 2). As a matter of fact, further Mössbauer studies of isomorphous $(Fe,Cd)_3(PO_4)_2$ and $(Fe,Ca)_3(PO_4)_2$ solid solutions together with this assignment indicate that $Cd^{2+}$ and $Ca^{2+}$ also concentrate in the M(1) sites (Nord and

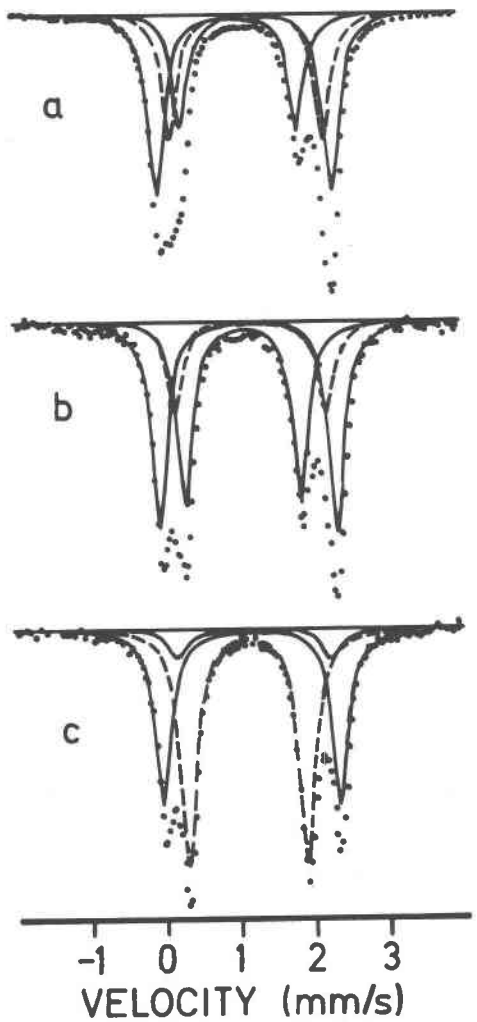


Fig. 2. Mössbauer spectra of (a) $(Fe_{0.90}Mn_{0.10})_3(PO_4)_2$, (b) $(Fe_{0.60}Mn_{0.40})_3(PO_4)_2$, and (c) $(Fe_{0.30}Mn_{0.70})_3(PO_4)_2$, all recorded at 295 K. The lines represent the individual Lorentzian doublets obtained in the computer fittings. In each of the spectra one Lorentzian doublet is dashed to make assignment easier.

Ericsson, manuscript), which is logical considering their radii. Moreover, X-ray diffraction studies of the graftonite $(Fe_{0.60}Mn_{0.27}Ca_{0.13})_3(PO_4)_2$ (Calvo, 1968) and the isostructural compound $Cd_2Zn(PO_4)_2$ (Calvo and Stephens, 1967) both indicate that the largest cations preferred the M(1) sites of the structure.

### Neutron diffraction study of $(Fe_{0.50}Mn_{0.50})_3(PO_4)_2$

In order to confirm the cation site assignment based on the Mössbauer investigation, a neutron powder diffracton study of $(Fe_{0.50}Mn_{0.50})_3(PO_4)_2$ was undertaken. Neutron data are favorable in this case because of the widely divergent scattering amplitudes for the metals: $b$(Fe) = +0.96 and $b$(Mn) = −0.36 (in $10^{-12}$ cm units). Using the site occupancies calculated from the Mössbauer data, the scattering amplitudes for the three cation sites in $(Fe_{0.50}Mn_{0.50})_3(PO_4)_2$ would be $b_1 = -0.19$, $b_2 = +0.33$, and $b_3 = +0.10$. According to the Mössbauer analysis $b_1$ is assigned to M(1), and so on. This assignment was to be verified using the neutron diffraction data.

Only data for $2 \leq \theta \leq 27°$ were used, including 130 independent reflections. For $\theta > 27°$ the reflections overlapped considerably, and it was impossible to define the background level. After subtraction of the background from the intensity profile, the net intensities were processed by means of the full-profile refinement procedure of Rietveld (1969). In a preliminary step the scale factor, zero point, and unit cell dimensions were refined, thus fixing the mean neutron wavelength at 1.5594(4)Å. The complete structure was then refined with 46 parameters: one overall scale factor, three peak profile parameters, 39 atomic coordinates and, to keep the number of parameters within reasonable limits, three isotropic temperature factors (for metals, phosphorus, and oxygen). The structural data for $Fe_3(PO_4)_2$ (Kostiner and Rea, 1974) were used as starting parameters. The $R_I$ value for the Möss-

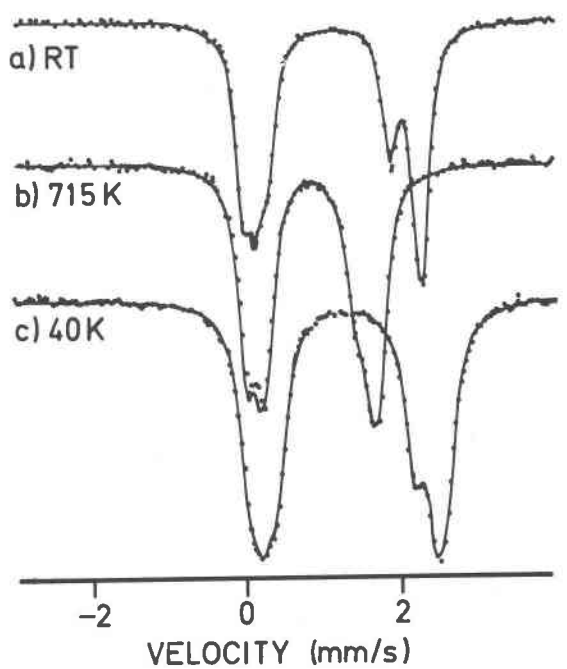


Fig. 3. Mössbauer spectra of $Fe_3(PO_4)_2$ recorded at different temperatures: (a) at room temperature (~295 K), (b) at 715 K, and (c) at 40 K. The full lines denote the sum of the computer-fitted Lorentzian functions.

Table 3. Some critical data from the six powder neutron-diffraction full-profile refinements

| No. | Scattering amplitude[a] M(1) | M(2) | M(3) | $R_I$ | Average σ(xyz)[b] (Fe,Mn) | P | O | Temperature factors (Å$^2$) $B$(Fe,Mn) | $B$(P) | $B$(O) |
|---|---|---|---|---|---|---|---|---|---|---|
| 1 | $b_1$ | $b_2$ | $b_3$ | 0.069 | 0.008 | 0.004 | 0.004 | -3.9(6) | 1.2(6) | 0.0(3) |
| 2 | $b_1$ | $b_3$ | $b_2$ | 0.197 | 0.032 | 0.009 | 0.008 | -3(2) | 6(2) | 1(1) |
| 3[c] | $b_2$ | $b_1$ | $b_3$ | (0.292) | 0.3 | 0.014 | 0.014 | >100 | -1(2) | 1(1) |
| 4 | $b_2$ | $b_3$ | $b_1$ | 0.150 | 0.098 | 0.008 | 0.007 | 16(20) | -2(1) | 0(1) |
| 5 | $b_3$ | $b_2$ | $b_1$ | 0.078 | 0.009 | 0.004 | 0.005 | -8.5(6) | 2.4(9) | 1.3(4) |
| 6 | $b_3$ | $b_1$ | $b_2$ | 0.270 | 0.163 | 0.012 | 0.014 | 50(18) | -3(2) | 0(2) |

*The estimated standard deviations given within parentheses refer to the last digit(s) of the respective values.*

a) *The metal scattering amplitudes are* $b_1 = -0.19$, $b_2 = 0.33$, *and* $b_3 = 0.10$
b) *"Average σ(xyz)" represents the grand mean of the standard errors of the respective atomic coordinates*
c) *This refinement did not converge*

bauer model converged to 0.069 after ten cycles of refinement ($R_p = 0.11$, $R_{wp} = 0.13$). The five other possible ways to combine metal scattering amplitudes and cation sites were then tested in the same way (Table 3).

The data of Table 3 favor No. 1[$b_1$ to M(1), $b_2$ to M(2), and $b_3$ to M(3)] as the correct model, in agreement with the Mössbauer analysis. The second best refinement (No. 5 in Table 3) implied impossible metal–oxygen bond distances, and the four other refinements clearly indicate that the respective cation assignments are not correct. The observed and calculated neutron data profiles for refinement No. 1 are shown in Figure 4. The atomic positional parameters from this refinement are listed in Table 4. The large standard deviations obtained for some coordinates are a consequence of the large number of parameters in the refinement and the small metal scattering amplitudes, which considerably reduce the accuracy. A table of the observed and calculated integrated intensities from the neutron diffraction refinement (the $b_1b_2b_3$ "Mössbauer" model) is available.[1]

## Discussion

The $Fe_3(PO_4)_2$ structure is built up of distorted $M(1)O_6$ octahedra sharing edges in pairs and arranged in sheets throughout the structure. Edge-sharing $M(3)O_5$ polyhedra form chains almost perpendicular to these sheets, while the $M(2)O_5$ polyhedra are joined to the sheets through corner-sharing. Illustrative figures of the structure type have been published earlier (Kostiner and Rea, 1974; Calvo, 1968). Some averaged interatomic distances and angles for $(Fe_{0.50}Mn_{0.50})_3(PO_4)_2$ are summarized in

[1] To obtain a copy of this table, order Document AM-82-199 from the Business Office, Mineralogical Society of America, 2000 Florida Avenue, N.W., Washington, D.C. 20009. Please remit $1.00 in advance for the microfiche.

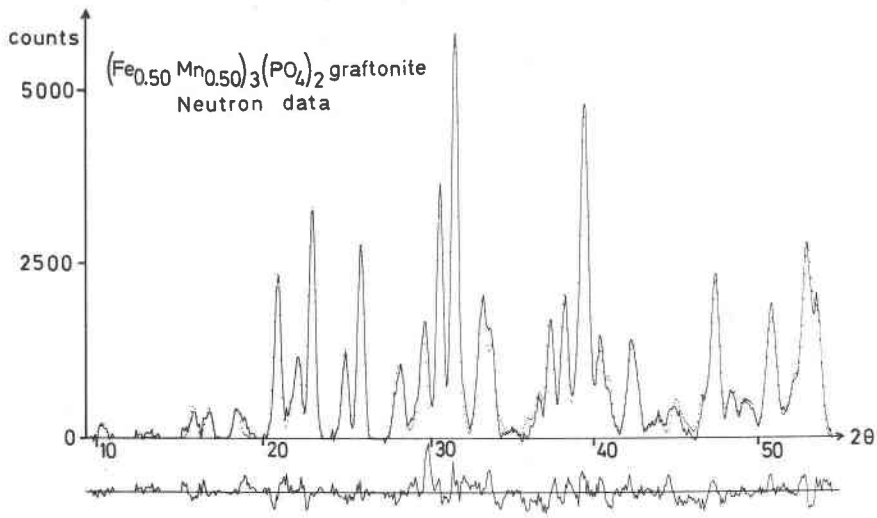


Fig. 4. The least-squares fit obtained between the observed intensities (continuous line) and calculated intensities (points) for $(Fe_{0.50}Mn_{0.50})_3(PO_4)_2$ from the neutron-diffraction full-profile refinement No. 1 (see text). The discrepancy in the fit ($I_{obs} - I_{calc}$) is plotted below on the same scale.

Table 4. Atomic positional coordinates for $(Fe_{0.50}Mn_{0.50})_3(PO_4)_2$ according to refinment No. 1 in Table 3

| Atom | x | y | z |
|---|---|---|---|
| M(1) | 0.951(8) | 0.128(4) | 0.854(9) |
| M(2) | 0.735(4) | 0.058(3) | 0.314(7) |
| M(3) | 0.381(16) | 0.204(8) | 0.142(17) |
| P(1) | 0.083(5) | 0.146(3) | 0.379(6) |
| P(2) | 0.621(4) | 0.100(3) | 0.806(5) |
| O(1) | 0.078(4) | 0.060(2) | 0.147(4) |
| O(2) | 0.471(3) | 0.194(3) | 0.811(4) |
| O(3) | 0.923(3) | 0.188(3) | 0.382(4) |
| O(4) | 0.720(4) | 0.112(2) | 0.613(5) |
| O(5) | 0.233(4) | 0.232(2) | 0.335(5) |
| O(6) | 0.701(3) | 0.081(2) | 0.018(4) |
| O(7) | 0.153(4) | 0.056(2) | 0.601(4) |
| O(8) | 0.527(3) | -0.051(3) | 0.760(4) |

*Estimated standard deviations are given in parentheses*

Table 5. Average interatomic distances (Å) and average angles for three graftonite-type structures

| | Fe..[a] | $Fe_{0.50}Mn_{0.50}$..[b] | $Fe_{0.60}Mn_{0.27}Ca_{0.13}$..[c] |
|---|---|---|---|
| M(1)-O | 2.231(4) | 2.37(7) | 2.43(2) |
| M(2)-O | 2.134(4) | 2.00(5) | 2.14(2) |
| M(3)-O | 2.101(4) | 2.03(9) | 2.16(2) |
| P(1)-O | 1.534(4) | 1.61(6) | 1.55(2) |
| P(2)-O | 1.535(4) | 1.62(6) | 1.55(2) |
| O-P(1)-O | 109.5°(2) | 109°(1) | 110°(1) |
| O-P(2)-O | 109.4°(2) | 109°(2) | 110°(1) |

*The coordination numbers for M(1), M(2), M(3), P(1), and P(2) are 6, 5, 5, 4, and 4, respectively, except for the graftonite mineral (c), where M(1) is 7-coordinated*

a) *Fe.. denotes $Fe_3(PO_4)_2$ and the values are from Kostiner and Rea (1974)*

b) *$Fe_{0.50}Mn_{0.50}$.. denotes $(Fe_{0.50}Mn_{0.50})_3(PO_4)_2$ and the values are from this work (neutron diffraction study No. 1)*

c) *$Fe_{0.60}Mn_{0.27}Ca_{0.13}$.. denotes graftonite $(Fe_{0.60}Mn_{0.27}Ca_{0.13})_3(PO_4)_2$ and the values are from Calvo (1968)*

*Estimated standard deviations are given in parentheses*

Table 5, with corresponding values for $Fe_3(PO_4)_2$ and Calvo's (1968) graftonite added for comparison. The somewhat inaccurate atomic positional parameters from our neutron diffraction study resulted in large standard deviations in the distances and improbably large P–O mean distances. In spite of these effects, it can be concluded that the mean metal–oxygen distance is significantly longer for M(1) than for M(2) and M(3) in $(Fe_{0.50}Mn_{0.50})_3(PO_4)_2$ as well as in $(Fe_{0.60}Mn_{0.27}Ca_{0.13})_3(PO_4)_2$. This reflects the larger cations ($Mn^{2+}$ and $Ca^{2+}$) preferentially occupying the M(1) sites, thus causing a significant increase in the M(1)–O distances with respect to $Fe_3(PO_4)_2$. The preference of $Mn^{2+}$ for the M(1) site is also in accordance with the interpretation of the Mössbauer data. Furthermore, $\Delta E_Q$ as well as CS decrease in a pronounced way for M(1) as the Mn content increases from $x = 0.7$ to $x = 0.9$ (Table 2). The unit cell volume also increases in a more pronounced way in the same interval (Fig. 1). We attribute this effect to substantial distortions especially in the $M(1)O_6$ polyhedra, thus making the structure less stable for higher Mn contents.

The fractional amounts of iron in the three distinct cation sites are displayed in Figure 5. The preference of $Mn^{2+}$ for the six-coordinated site is in agreement with many other crystallographic observations. High-spin $Mn^{2+}$ receives zero crystal-field stabilization energy in an octahedral environment of oxygen ligands, and its structural role is therefore controlled principally by local electric charge and size effects (Peacor, 1978). Cation distribution studies have shown that relative to $Fe^{2+}$, the $Mn^{2+}$ ion usually occupies the largest site. Furthermore, $Fe^{2+}$, somewhat more strongly than $Mn^{2+}$, seems to prefer distorted sites (Peacor, 1978; Ghose, 1978). This is again in accordance with our results. There is also a difference between the two five-coordinated sites in the $(Fe,Mn)_3(PO_4)_2$ solid solutions: $Fe^{2+}$ somewhat prefers the M(2) "square pyramid" sites to the M(3) "trigonal bipyramid" sites, while the converse is true for $Mn^{2+}$. It is uncertain, though, whether this dependence is caused by a size effect, the slightly different cationic environments, or the fact that $M(2)O_5$ is more distorted than $M(3)O_5$ judged from the variations in the metal-oxygen distances. Finally, it is noteworthy that for M(3), the atomic fraction $X_{Fe}$ depends almost linearly on the total amount of iron in each phase.

In cation studies involving two kinds of cations and two non-equivalent cation sites, it is customary

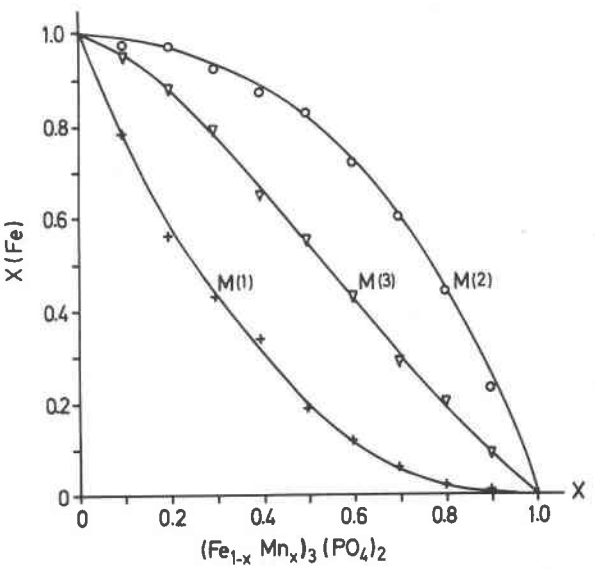


Fig. 5. Site occupancies for $Fe^{2+}$ ($X_{Fe}$) at the M(1), M(2) and M(3) sites of $(Fe_{1-x}Mn_x)_3(PO_4)_2$ ($0 \leq x \leq 0.9$) according to the Mössbauer analyses.

to calculate a cation distribution coefficient, $K_D$, for the intra-crystalline cation exchange reaction. In the present $(Fe,Mn)_3(PO_4)_2$ phases we have combined the five-coordinated sites M(2) and M(3) and thus defined a distribution among five- and six-coordinated sites with the expression

$$K_D' = (X^V_{Fe} \cdot X^{VI}_{Mn})/(X^{VI}_{Fe} \cdot X^V_{Mn}),$$

where V and VI denote the coordination numbers. Our nine phases gave an average of $K_D' \approx 10$, which more explicitly describes the stronger $Fe^{2+}$ preference for five-coordination. A comparison may be made with a purely hypothetical $(Fe,Mn)_3(PO_4)_2$ phase with the farringtonite structure (*i.e.*, isostructural with $Mg_3(PO_4)_2$ and "$\gamma$-$Zn_3(PO_4)_2$"), containing five- and six-coordinated divalent cations. In a study of such $(Mg_{1-x}Me_x)_3(PO_4)_2$ solid solutions (Nord and Stefanidis, 1980), the distribution factor $K_D = (X^V_{Me} \cdot X^{VI}_{Mg})/(X^{VI}_{Me} \cdot X^V_{Mg})$ was determined for $Mg^{2+}/Fe^{2+}$ ($K_D = 1.4$) and for $Mg^{2+}/Mn^{2+}$ ($K_D \approx 0.3$). If the $K_D$ factor is supposed to represent the equilibrium constant of the exchange reaction

$$Me^{2+}\ (VI) + Mg^{2+}\ (V) \rightleftarrows Me^{2+}\ (V) + Mg^{2+}\ (VI)\ [Me = Fe \text{ or } Mn],$$

a hypothetical $Fe^{2+}/Mn^{2+}$ distribution factor in this structure type may be derived by combining the two respective equilibrium equations, giving $K_D \approx 5$ (*i.e.*, 1.4/0.3), which may be compared with the above cited value of $K_D'$ for the graftonite structure type. An extensive study of several other $(Fe_{1-x}Me_x)_3(PO_4)_2$ solid solutions is in progress (Nord and Ericsson, manuscript) in order to define solid solution relationships in such structures.

## Acknowledgments

We are grateful to Dr. Hans Annesten, University of Uppsala, and Dr. Bengt Lindqvist, Swedish Museum of Natural History, for their critical reading of the manuscript. Professor Eric Welin, also at the Swedish Museum, is cordially thanked for the excellent laboratory and computing facilities placed at our disposal. We are also indebted to Dr. Roland Tellgren, University of Uppsala, for his willing help during the collection of neutron diffraction data. The generous financial support from the Swedish Natural Science Research Council is gratefully acknowledged.

## References

Annersten, H., Ericsson, T. and Nord, A. G. (1980) The cation ordering in iron-containing zinc and magnesium orthophosphates determined from Mössbauer spectroscopy. Journal of the Physics and Chemistry of Solids, 41, 1235–1240.

Bancroft, G. M. (1973) Mössbauer Spectroscopy: An Introduction for Inorganic Chemists and Geochemists. McGraw-Hill, London.

Calvo, C. (1963) The crystal structure and luminescence of $\gamma$-zinc orthophosphate. Journal of the Physics and Chemistry of Solids, 24, 141–149.

Calvo, C. (1968) The crystal structure of graftonite. American Mineralogist, 53, 742–750.

Calvo, C. and Stephens, J. S. (1968) Crystal structure of $CdZn_2(PO_4)_2$ and $Cd_2Zn(PO_4)_2$. Canadian Journal of Chemistry, 46, 903–915.

Clark, M. G., Bancroft, G. M. and Stone, A. J. (1967) Mössbauer spectrum of $Fe^{2+}$ in a square-planar environment. Journal of Chemical Physics, 47, 4250–4261.

DuFresne, E. R. and Roy, S. K. (1961) A new phosphate mineral from the Springwater pallasite. Geochimica et Cosmochimica Acta, 24, 198–205.

Ghose, S. (1978) Iron: crystal chemistry. In K. H. Wedepohl, Ed., Handbook of Geochemistry, Vol. II/3, Chapter 26-A. Springer-Verlag, Berlin-Heidelberg.

Ingalls, R. (1964) Electric-field gradient tensor in ferrous compounds. Physical Review, 133A, 787–795.

Kostiner, E. and Rea, J. R. (1974) Crystal structure of ferrous phosphate, $Fe_3(PO_4)_2$. Inorganic Chemistry, 13, 2876–2880.

Mattievich, E. and Danon, J. (1977) Hydrothermal synthesis and Mössbauer studies of ferrous phosphates of the homologous series $Fe_3(PO_4)_2(H_2O)_n$. Journal of Inorganic and Nuclear Chemistry, 39, 569–580.

Nord, A. G. (1977) The cation distribution in $Zn_2Mg(PO_4)_2$ determined by X-ray profile-fitting refinements. Materials Research Bulletin, 12, 563–568.

Nord, A. G. and Kierkegaard, P. (1968) The crystal structure of $Mg_3(PO_4)_2$. Acta Chemica Scandinavica, 22, 1466–1474.

Nord, A. G. and Kierkegaard, P. (1980) Crystal chemistry of some anhydrous divalent-metal phosphates. Chemica Scripta, 15, 27–39.

Nord, A. G. and Stefanidis, T. (1980) The cation distribution between five- and six-coordinated sites in some $(Mg,Me)_3(PO_4)_2$ solid solutions. Materials Research Bulletin, 15, 1183–1191.

Peacor, D. R. (1978) Manganese: crystal chemistry. In K. H. Wedepohl, Ed., Handbook of Geochemistry, Vol. II/3, Chapter 25-A. Springer-Verlag, Berlin-Heidelberg.

Rietveld, H. M. (1969) A profile refinement method for nuclear and magnetic structures. Journal of Applied Crystallography, 2, 65–71.

Stephens, J. S. (1967) Crystallography of $(Zn,Cd,Mn)_3(PO_4)_2$ Compounds. Ph. D. Thesis, McMaster University, Hamilton (Ontario)

Stephens, J. S. and Calvo, C. (1969) Crystal structure of $\beta'$-$Mn_3(PO_4)_2$. Canadian Journal of Chemistry, 47, 2215–2225.

Stephenson, D. A. and Moore, P. B. (1968) The crystal structure of grandidierite, $(Mg,Fe)Al_3SiBO_9$. Acta Crystallographica, B24, 1518–1522.

Tang Kai, A., Annersten, H. and Ericsson, T. (1980) Molecular orbital MSX$\alpha$ calculations of *s*-electron densities of tetrahedrally coordinated ferric iron: comparison with experimental isomer shifts. Physics and Chemistry of Minerals, 5, 343–349.

*Manuscript received, September 14, 1981; accepted for publication, January 4, 1982.*